applied optics

Focus-tunable low-power electrowetting lenses with thin parylene films

Alexander M. Watson,[1,*] Kevin Dease,[2] Soraya Terrab,[1] Christopher Roath,[3] Juliet T. Gopinath,[2] and Victor M. Bright[1]

[1]Department of Mechanical Engineering, University of Colorado Boulder, Boulder, Colorado 80309, USA
[2]Department of Electrical, Computer and Energy Engineering, University of Colorado Boulder, Boulder, Colorado 80309, USA
[3]VSI Parylene, Louisville, Colorado 80027, USA
*Corresponding author: alexander.m.watson@colorado.edu

Received 13 April 2015; revised 18 June 2015; accepted 19 June 2015; posted 19 June 2015 (Doc. ID 237971); published 8 July 2015

Electrowetting lenses with record low power consumption (microwatts) have been demonstrated using high-quality parylene AF-4 dielectric layers and large dodecyl sulfate ions. Water and propylene glycol are interchanged as the polar liquid to enable diverging and converging lens operation achievable with the application of 15 V. The optical quality of the lenses is comparable to conventional microlenses and the tuning exhibits very little (<0.5°) contact angle hysteresis.

OCIS codes: (220.1080) Active or adaptive optics; (220.3620) Lens system design; (220.3630) Lenses.

http://dx.doi.org/10.1364/AO.54.006224

1. INTRODUCTION

Electrowetting liquid lenses have been studied for over a decade [1] because they offer great promise as adaptive optical devices. They provide an attractive, compact solution with no moving parts, millisecond response times [2,3], polarization insensitivity, tuning ranges over hundreds of diopters [4–6], and optical quality comparable to solid microlenses [4,7]. Simple voltage actuation allows for robust and compact devices compared to optofluidic tunable lenses controlled with external microfluidics [8]. Flexible membrane liquid lenses without periphery components have been demonstrated with comparable voltages and tuning ranges [9–11], but have yet to be demonstrated as individually addressable arrays like electrowetting devices [6,12]. We have demonstrated electrowetting liquid lenses tunable from −43.5 to 0 diopters with 15 V DC and a power consumption of 25 μW, the lowest reported to the best of our knowledge. By using thin, high-quality dielectric layers and a large ion source, we can reduce the voltage and power requirements of electrowetting lens devices.

Electrowetting is a phenomenon in which an applied voltage changes the shape of a liquid droplet. The surface energy balance between droplet, substrate, and surrounding medium determines the contact angle of the droplet, by Young's equation

$$\cos\theta_Y = \frac{\gamma_{SV} - \gamma_{SL}}{\gamma_{LV}}, \tag{1}$$

where θ is the contact angle, γ is the surface tension, and S, L, and V represent the surface, liquid, and vapor media, respectively. By applying a voltage between the conductive droplet and electrode separated by a thin film dielectric, charges build up on the droplet surface above the electrode. The buildup of charge produces a force on the droplet at the three phase contact line that directly opposes the surface tension force between the droplet and substrate [13]. To balance the surface tension with this electric force, the effective contact angle decreases, following the Lippmann–Young equation,

$$\cos\theta = \cos\theta_Y + \frac{\epsilon_D\epsilon_0}{2d\gamma_{LV}}v^2, \tag{2}$$

where $\epsilon_D\epsilon_0$ represents the permittivity of the dielectric separating the droplet from the electrode, d is the dielectric thickness, v represents the applied voltage, and θ is the new contact angle. In a cylindrical cavity filled with two liquids, as seen in Fig. 1, the focal length of the lens formed by the meniscus can be derived from the contact angle with the thin-lens approximation as

$$\frac{1}{f} = \frac{-\cos(\theta)}{r}\cdot\left(\frac{n_1}{n_2} - 1\right), \tag{3}$$

where r is the radius of the cylindrical cavity, and n_1 and n_2 are the indices of refraction of the polar and nonpolar liquid, respectively. Figure 1 shows how a capillary tube with sidewall electrodes, a thin film dielectric, and a hydrophobic layer can be filled with the polar and nonpolar liquids to realize a focus-tunable lens based on contact angle change from electrowetting.

To maintain charge buildup on the sidewall, a dielectric layer is needed to separate the polar liquid and electrode.

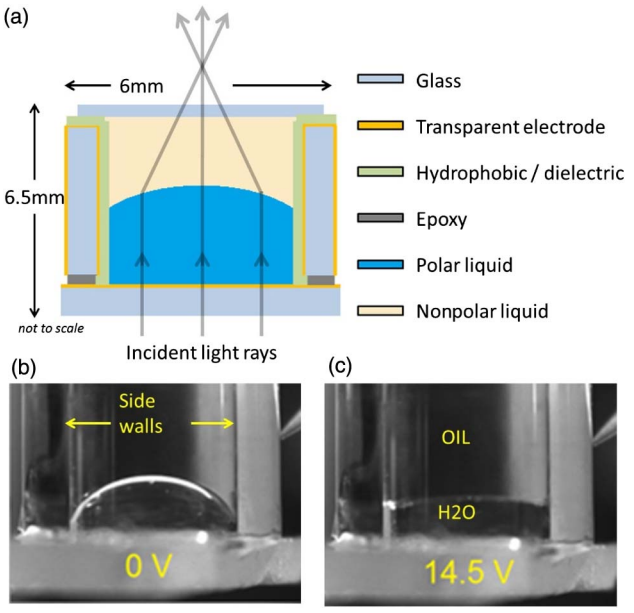

Fig. 1. (a) Cross-section view of electrowetting liquid lens device. A glass capillary tube is coated with IZO electrode, parylene AF-4 dielectric, and Teflon hydrophobic coating. The substrate ITO glass is bonded with epoxy, and a coverslip seals the device. (b) Side view images of the liquid lens tuning from its initial curved state to (c) flat with the application of 14.5 V.

This charge pulls the droplet's edge up the sidewall while surface tension forces maintain a spherical surface across the lens. The resulting contact angle and therefore focal length of the lens is dependent on the voltage applied, as per Eqs. (1) and (2). It is important to eliminate ion leakage through the dielectric to ensure reliable tuning. The resistance of ion injection in thin-film parylene AF-4 (also known as parylene HT) dielectrics for electrowetting [14] combined with an ion source containing long alkane chains [15] mitigates charge diffusion through the dielectric. These attributes allow for devices with little hysteresis while tuning and extremely low power consumption caused by leaked charge. Consequently, the dielectric thickness can be reduced from the typical 1 μm thickness to a few hundred nanometers while maintaining reliable tuning. This is desirable since a thinner dielectric reduces the voltage necessary for electrowetting actuation. As a result, we enable lenses with >40 diopter tuning range with 15 V applied. Our voltage of 15 V is significantly lower than typical values of ~50–250 V [1,4,5] for electrowetting. In addition, the low voltages of our device enable thin-film transistor control and subsequent integration of adaptive optics with arrayed, on-chip microsystems [16].

2. FABRICATION

The liquid lens device seen in Fig. 1 is formed at the boundary between the polar liquid (water, propylene glycol) and the nonpolar liquid (dodecane oil). The liquids are contained within a glass capillary tube, sealed by a glass substrate and coverslip. The substrate and sidewall electrodes are chosen to be indium tin oxide (ITO) and indium zinc oxide (IZO), respectively, due to their optical transparency. Selection of parylene AF-4 (also known as parylene HT) instead of the standard parylene C as the dielectric layer is essential in allowing for the 300 nm thin film to resist dielectric failure and charge injection [14].

The liquid lens is contained within a glass tube of 2.7 mm inner diameter and 6 mm outer diameter. The tube is cut to a height of 5 mm. The IZO sidewall electrode is sputter coated to form a continuous film from inside to outside of the capillary tube. To ensure minimal defects and good conductivity of the film, the sputter chamber is pumped to a base pressure of 1 μT. The sputter is performed in an argon environment at an operating pressure of 8 mT to reduce the mean free path within the chamber to lengths much shorter than the distance between target and sample. This helps to produce a continuous, conformal coating that covers the outer sidewall, inner sidewall, and top of the cylindrical cavity [17]. The IZO deposition is run at 120 W for 12 min, producing a 200 nm thin film. A multimeter is used to confirm electrical connection from inside to outside of the lens device, and the resistivity of the thin film is measured to be 1.7 mΩ · cm. The outside of the lens device is masked with Kapton tape for subsequent dielectric and hydrophobic coating depositions.

A commercial coatings company, VSI Parylene, deposited the dielectric film of 300 nm parylene AF-4 according to the Gorham process [18]. Parylene AF-4 is fluorinated, whereas parylene C contains a Cl atom attached to the benzene ring. Due to its dipole moment, the chlorinated parylene C monomer readily condenses onto substrates in the vacuum chamber while the parylene AF-4 monomer requires more surface energy change for condensation. This affords the parylene AF-4 monomer more penetrating power than parylene C, and allows it to conform to complex geometries more readily than parylene C. The high surface conformity of parylene AF-4 allows it to form quasi-pinhole-free films at a lower thickness than parylene C [19].

A hydrophobic layer of 1:20 solution of Dupont's Teflon AF1600:Fluorinert FC-40 is added over the parylene AF-4 layer. While parylene AF-4 has been shown to be hydrophobic [14], we found that the Teflon top coat is more effective for eliminating droplet pinning points on the surface. The Teflon AF1600 is dip-coated and cured at 125°C for 10 min, followed by a cure at 170°C for 25 min. The adhesion of the cured Teflon to the parylene AF-4 is tested by tape exfoliation and resulted in no delamination. The Kapton tape is removed to expose an electrical connection to the inner sidewall. The bottom substrate used for the lens is a commercial grade ITO-coated glass substrate with a 4–10 Ω · cm film on one side to electrically address the polar liquid. The substrate is bonded to the cylinder using Masterbond EP30-2 in order to ensure a leak-proof enclosure that resists liquid permeation and isolates the substrate electrode from the sidewall electrode.

The lenses are filled with a micropipette using dodecane oil (Sigma-Aldrich, $n = 1.420$) and either water-based ($n = 1.333$) or propylene glycol-based (Sigma-Aldrich, $n = 1.432$) polar liquid. The liquid refractive indices were measured with a refractometer. Two different polar liquids are selected to enable diverging or converging lensing. To create a diverging lens, a 1% sodium dodecyl sulfate (SDS, Sigma-Aldrich) in DI water

solution is used. A 1% SDS in propylene glycol solution is used to enable converging lens operation. In addition to reducing the surface tension between the polar liquid and oil, the SDS provides a large, negatively charged dodecyl sulfate ion, which cannot easily penetrate the parylene layer [15].

The SDS ionic molecule has a total radius of 1.75 nm, with the sodium ion accounting for 0.227 nm [20]. Thus, the dodecyl sulfate ion with a long alkane chain is much larger than the typical ionic salt ions used in the working polar fluid. This greatly reduces the leakage current generated by ion transport through the dielectric layer. This lowers the power consumption during operation and enhances the lens reliability by preventing hysteresis associated with charge injection in the dielectric. The quality of the parylene AF-4 also allows for a quasi-pinhole-free thin layer down to 200 nm [21]. The practical limit to lowering electrowetting voltage by reducing dielectric thickness is dependent on the leakage of ions through the dielectric that, in excess, causes electrolysis and device failure. By combining large ions with high-quality dielectrics, such as parylene AF-4 or atomic layer deposited oxides [16], the voltage requirement for reliable electrowetting can be scaled down with dielectric thickness to levels much lower than previous electrowetting lens devices.

A 0.17 mm thin glass coverslip seals the lens device. At this scale, surface tension forces dominate over forces of gravity [22]. Previous simulations on 2 mm diameter droplets show that gravity has a negligible effect on the surface profile, causing only $\lambda/50$ deviation from a spherical profile, and predict that with density-matched liquids, larger dimensions of lenses are possible [23]. The surface tension of the oil holds the coverslip in place when operating sideways or upside down.

3. LENS CHARACTERIZATION

A. Diverging Lens

Optical power performance measured at 780 nm and hysteresis of the water-based lens can be seen in Fig. 2. By applying negative voltage to the polar liquid, we ensure that the large dodecyl sulfate ions are attracted to the sidewall with the dielectric. Application of −15 V DC tunes the liquid lens from resting power of −43 diopters to a flat liquid profile with 0 optical power. Continued voltage tuning to −30 V alters the optical power to +10 diopters, covering a focal length range of −23 mm through infinity and down to +100 mm.

The measured contact angle has very little hysteresis when tuning the device, averaging $< 0.5°$ when tuning to from 0 to −15 V and back. Inspection of the contact line around the inner circumference of the tube shows no sagging or pinned points of the polar liquid, indicating good homogeneity of the thin films. At ∼12 V we see the onset of contact angle saturation (CAS), which reduces and ultimately eliminates any further contact angle change with increased voltage. CAS is ubiquitous in most electrowetting experiments, and causes the contact angle response to deviate from the Lippmann–Young equation [22]. A comprehensive study by Chevalliot *et al.* [24] shows the invariance of contact angle saturation to a number of material parameters, such as dielectric thickness, liquid–liquid surface tension, ion size, and pH. At this time, there is no complete understanding in the electrowetting literature on what causes CAS. However, in our design, a marked difference in CAS is measured when the polar liquid in the lens is changed from water to propylene glycol. Results are plotted in Fig. 3.

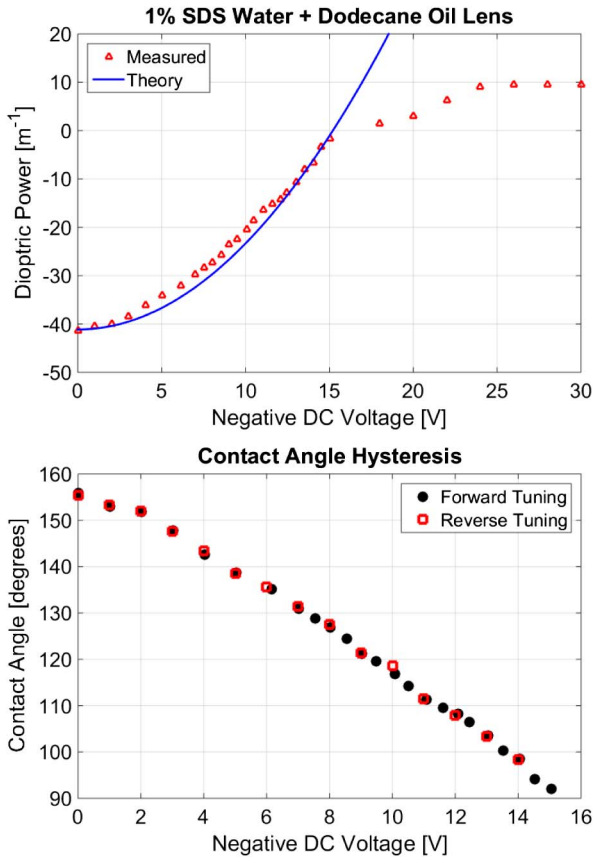

Fig. 2. Top: the dioptric power of the water-based lens agrees closely with theoretical values predicted by material properties and Lippmann–Young equation. The power tunes from −43 diopters to 0 diopters with the application of −15 V. Continued tuning realizes a positive lens up to +10 diopters before contact angle saturation. Bottom: plot of contact angle of the polar liquid with respect to the sidewall over the tuning range of the diverging water-based lens. Average hysteresis of each measured data point is <0.5° when tuning forward and back.

The same SDS concentration is used as the ion source for both types of lenses, but we see a 30 deg difference in saturation angle. The differences between water and propylene glycol that could contribute to this discrepancy are: molecular weight and size, the polar component of their surface tension value, and the work of adhesion force that holds like molecules together. Since the ion source and concentration are equal and the parylene AF-4 dielectric resist charge injection, it seems unlikely that this drastic difference in CAS is due to trapped charge alone. The differences in material properties between water and glycol suggest that material interactions between polar liquid and nonpolar liquid and/or substrate can have a large effect on CAS.

B. Converging Lens

The optical power tuning at 780 nm and electrical power consumption of the propylene glycol lens are shown in Fig. 4. Due to the relatively small refractive index contrast between

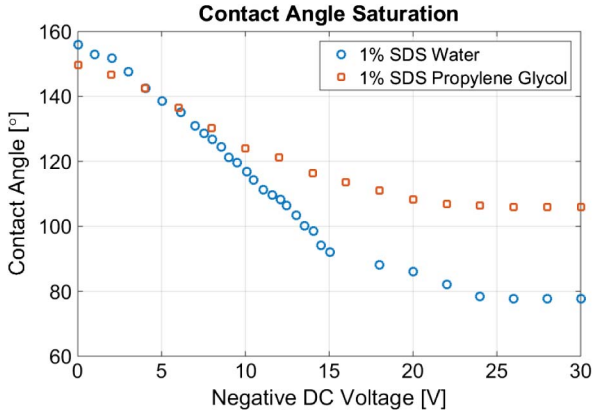

Fig. 3. Comparison of CAS between 1% SDS water + dodecane oil lens and 1% SDS propylene glycol + dodecane oil lens. An approximately 30 deg difference in saturation angle is observed between water- and glycol-based polar liquids.

propylene glycol ($n_d = 1.432$) and dodecane oil ($n_d = 1.420$), the change in lens power with applied voltage is smaller than the water and oil lens. This enables finer precision control of the lens at the cost of total tuning range. The converging lens tunes from +5.4 diopters to +2.5 diopters by applying −15 V. The effect of CAS is stronger with the glycol-based device, and occurs at the lower voltage of approximately −9 V. Continued tuning up to −30 V reduces the contact angle from 150 to 106 deg before full saturation, covering a focal length range of +185 to +580 mm.

The power consumption of the propylene glycol lens device ranges linearly between 0 and 25 μW while applying 0 to −15 V. This is an order of magnitude lower than previously reported DC voltage-based liquid lenses [1,4,25]. Low voltage and power requirements are crucial when integrating with chip scale microsystems, which is an attractive option for miniaturized variable optical devices, such as electrowetting lenses, prisms, and phase modulators [7].

C. AC versus DC Voltage Operation

The devices operate with the lowest power using DC voltage actuation since the steady-state power consumption is due only to leaked charge. However, at prolonged exposure to DC bias, the dielectric film will eventually take on enough charge to affect the contact angle causing challenges with wetting reversibility and hysteresis. With our devices under DC operation near saturation at 15 V, a constant electric field has a strength of the order of 0.4 MV/cm. While this is well below the breakdown threshold of the parylene AF-4 (5 MV/cm) [26], it remains as a driving force to inject ions into the dielectric. To test the effects of inevitable charge injection, one glycol-based device was charged to saturation voltage of 24 V DC (0.64 MV/cm) before removing the probes that connected the power supply. After 30 min unconnected, the contact angle relaxed 25 deg, marking a change in power of 2.6 diopters of the lens. Compare this rate of charge injection in parylene AF-4 to results from [24] with electrowetting on ITO/1.3 μm Parylene C/50 nm Fluoropel (hydrophobic coating). The electric field was only 0.29 MV/cm yet the same contact angle relaxation occurred within 60 s or less.

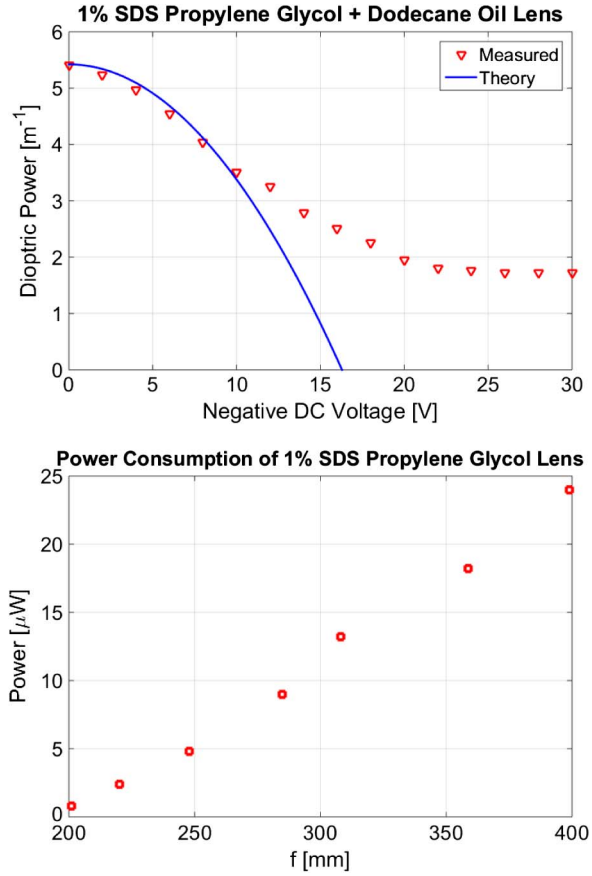

Fig. 4. Top: the focal length of the glycol-based converging lens agrees with theory until CAS onset at 10 V causes the response to begin to flatten out. The converging lens tunes from +5.4 diopters to +2.5 diopters with an applied voltage of −15 V. Increased tuning brings the power down to 1.7 diopters before full CAS. Bottom: plot of power consumption over focal length range for the glycol-based lens. 25 μW of power dissipation is observed with continuous operation while tuning with −15 V.

The advantage of using AC voltage to drive the lens actuation is that the alternating polarity of the voltage helps to eliminate charge injection that occurs from sustained DC bias. However, under AC voltage, the smaller sodium ions from the SDS are now part of the collection of ions building up at the dielectric surface during electrowetting. Thus we lose the advantage that the large dodecyl sulfate ion allowed and see bubble formation indicative of hydrolysis and device failure at 18 V_{rms}. The contact angle response of a glycol-based lens can be seen in Fig. 5.

The contact angle measurement above can be compared to Fig. 3 where the glycol lens was tuned with DC voltage. Note the dielectric thickness for the device in Fig. 5 is 370 nm, compared to the 300 nm from the devices measured in Fig. 3. Interestingly, the glycol-based lens tuned by AC voltage is able to surpass the CAS limit when tuned by DC voltage. This similar dependence on AC versus DC voltage is reported in [24], where AC voltages allow for further tuning before CAS sets in. Higher voltage tuning to experimentally investigate the CAS point for the glycol-based lens with AC tuning was not possible

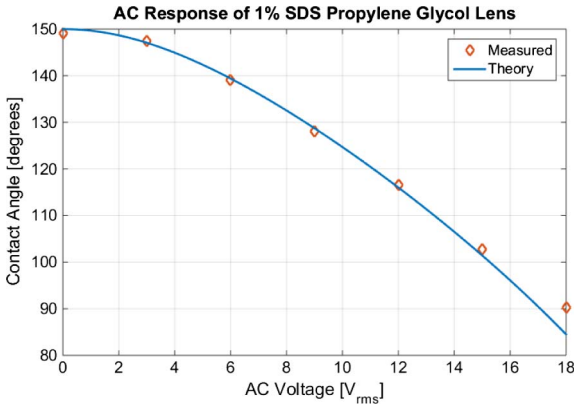

Fig. 5. Comparison of measured and theoretical contact angle of a propylene glycol-based lens operated with 100 Hz AC square wave voltage. This lens has a 370 nm thick parylene AF-4 layer. CAS begins to occur at 15 V_{rms}.

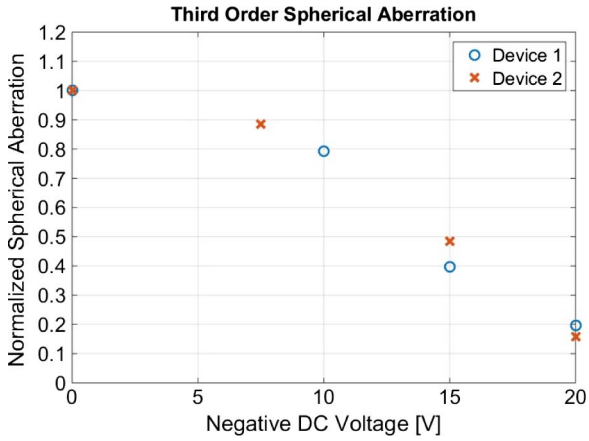

Fig. 6. Spherical aberration Zernike coefficients values are determined by fitting the wavefront to the third-order spherical aberration polynomial $6\rho^4 - 6\rho^2 + 1$. The wavefront is measured at various points while tuning the lens devices in the operating range between 0 and −20 V. Both devices depict the trend of decreasing spherical aberration magnitude as the lens is tuned from maximum curvature toward flat.

due to thin-film breakdown and device failure. This challenge can be addressed by using ion sources where both cation and anion are large so that AC tuning can be reliable in low-voltage electrowetting applications [15].

4. LENS QUALITY

It is important to quantify lens aberrations as a function of tuning. We characterized the lens operating in horizontal orientation (i.e., the normal to the lens parallel with the table) with a wavefront sensor and determined the RMS deviations from a perfect spherical wavefront and the Zernike polynomial coefficients. A spatially filtered and collimated 532 nm laser was used for the characterization. The beam has a diameter of 2.588 mm on its major axis and 2.327 mm on its minor axis, determined by a $1/e^2$ intensity threshold. The laser propagates through the glycol-based liquid lens and the resulting wavefront at the exit pupil of the lens was imaged onto a Shack–Hartmann μ-eye wavefront sensor (CLAS-2D with software from Lumetrics). The wavefront sensor measures the wavefront intensity and phase. To determine the RMS deviation from a sphere and Zernike coefficients, the phase data was masked with a 2.3 mm diameter circle. The mask eliminates edge effects and pixilation from the wavefront sensor. To verify the phase measurement procedure, a 200 μm pinhole was placed in the beam path and the phase of the wavefront was found to agree with theoretical predictions.

The RMS deviation from a spherical wavefront was calculated from the aberration function determined by subtracting a best-fit sphere. The average values of the RMS deviation ranged from 88.98 nm at 0 V to 217.49 nm at 20 V. This result is comparable to previously reported values for RMS wavefront errors in electrowetting lens systems of 80 nm [7] and 211 nm [25] and in elastomeric lenses of 400 nm [27]. Berge *et al.* report wavefront error values of the similarly sized, commercially available Varioptic lens A316 of 30–90 nm over the full tuning range, disregarding tilt and focus Zernike modes [28].

The Zernike polynomial coefficients for third-order spherical aberration were measured for two devices. The best-fit sphere was subtracted from the phase data and the resulting aberration function was fit to the Zernike polynomials. The third-order spherical aberration used for fitting is $6\rho^4 - 6\rho^2 + 1$, where ρ is the radial distance normalized to the Zernike circle [29]. Figure 6 illustrates the normalized spherical aberration Zernike coefficient for each device as the lenses are tuned from a small radius of curvature toward an infinite (flat) radius of curvature. The average measured spherical aberrations range from −92.21 nm at 0 V to −17.68 nm at 20 V.

The spherical aberrations grow smaller in magnitude as the lens is tuned from its highest curvature at 0 V toward a flatter lens profile as voltage is increased. This agrees with the general trend that lenses with shorter focal lengths have more pronounced effects from spherical aberration due to the higher lens curvature.

5. CONCLUSION

By taking advantage of the exceptional insulating properties of parylene AF-4 and the large ion size of SDS, we can enable reliable DC electrowetting on 300 nm thin films with low voltage tuning. The 15 V lens tuning is compatible with low-cost voltage drivers and does not require a voltage transformer to integrate with microsystems. Furthermore, the power consumption due to the leakage current during operation is reduced to tens of microwatts. These are important steps for integrating electrowetting lenses into microsystems that require low voltage, such as endoscopy, and low power draw, such as battery-powered mobile optical systems. Replacing water with propylene glycol as the polar liquid changes the sign of the lens power and has interesting effects on the contact angle saturation. A difference in 30 deg in saturation angle is significant considering the only change in the system is that the polar molecule solvent carrying the ions is H_2O in one case and $C_3H_8O_2$ in the other. This indicates that contact angle saturation is influenced by interactions involving the polar material and not

simply the ions within the material system. Further investigation of CAS for propylene glycol under AC voltage actuation experimentally confirmed a dependence on driving voltage type and saturation angle. Future work on this topic will include a thorough investigation of the effects of polar materials on CAS.

Funding. National Science Foundation (NSF) (DBI-1353757).

Acknowledgment. The authors would like to acknowledge technical assistance from Professor Robert McLeod, Martha Bodine, Robert Niederriter, Professor Robert Cormack, and David Glugla.

REFERENCES

1. B. Berge and J. Peseux, "Variable focal lens controlled by an external voltage: an application of electrowetting," Eur. Phys. J. **3**, 159–163 (2000).
2. N. R. Smith, L. Hou, J. Zhang, and J. Heikenfeld, "Experimental validation of >1 kHz electrowetting modulation," in *University/Government/Industry Micro/Nano Symposium*, Louisville, Kentucky, 2008, pp. 11–14.
3. C. U. Murade, D. van den Ende, and F. Mugele, "High speed adaptive microlens array," Opt. Express **20**, 18180–18187 (2012).
4. F. Krogmann, W. Moench, and H. Zappe, "A MEMS-based variable micro-lens system," J. Opt. A **8**, S330 (2006).
5. S. Kuiper and B. H. Hendriks, "Variable-focus liquid lens for miniature cameras," Appl. Phys. Lett. **85**, 1128–1130 (2004).
6. N. R. Smith, L. Zhou, J. Zhang, and J. Heikenfeld, "Fabrication and demonstration of electrowetting liquid lens arrays," J. Display Technol. **5**, 411–413 (2009).
7. R. D. Niederriter, A. M. Watson, R. N. Zahreddine, C. J. Cogswell, R. H. Cormack, M. V. Bright, and J. T. Gopinath, "Electrowetting lenses for compensating phase and curvature distortion in arrayed laser systems," Appl. Opt. **52**, 3172–3177 (2013).
8. N.-T. Nguyen, "Micro-optofluidic lenses: a review," Biomicrofluidics **4**, 031501 (2010).
9. K. Wei, N. W. Domicone, and Y. Zhao, "A tunable liquid lens driven by concentric annular electroactive actuator," in *2014 27th IEEE International Conference on Micro Electro Mechanical Systems (MEMS)*, San Francisco, California, 2014.
10. A. Pouydebasque, C. Bridoux, F. Jacquet, S. Moreau, E. Sage, D. Saint-Patrice, C. Bouvier, C. Kopp, G. Marchand, S. Bolis, N. Sillon, and E. Vigier-Blanc, "Varifocal liquid lenses with integrated actuator, high focusing power and low operating voltage fabricated on 200 mm wafers," Sens. Actuators A **172**, 280–286 (2011).
11. S. Nicolas, M. Allain, C. Bridoux, S. Fanget, S. Lesecq, M. Zarudniev, S. Bolis, A. Pouydebasque, and F. Jacquet, "Fabrication and characterization of a new varifocal liquid lens with embedded pzt actuators for high optical performances," in *2015 28th IEEE International Conference on Micro Electro Mechanical Systems (MEMS)*, Estoril, Portugal, 2015.
12. Y. Kwon, Y. Choi, K. Choi, Y. Kim, S. Choi, J. Lee, and J. Bae, "Development of micro variable optics array," in *2014 27th IEEE International Conference on Micro Electro Mechanical Systems (MEMS)*, San Francisco, California, 2014.
13. T. B. Jones, "More about the electromechanics of electrowetting," Mech. Res. Commun. **36**, 2–9 (2009).
14. M. Dhindsa, S. Kuiper, and J. Heikenfeld, "Reliable and low-voltage electrowetting on thin parylene films," Thin Solid Films **519**, 3346–3351 (2011).
15. B. Raj, M. Dhindsa, N. R. Smith, R. Laughlin, and J. Heikenfeld, "Ion and liquid dependent dielectric failure in electrowetting systems," Langmuir **25**, 12387–12392 (2009).
16. J. Heikenfeld, N. Smith, M. Dhindsa, K. Zhou, M. Kilaru, L. Hou, J. Zhang, E. Kreit, and B. Raj, "Recent progress in arrayed electrowetting optics," Opt. Photon. News **20**, 20–26 (2009).
17. M. J. Madou, *Fundamentals of Microfabrication* (CRC Press, 2002).
18. W. F. Gorham, "A new, general synthetic method for the preparation of linear poly-p-xylylenes," J. Polym. Sci. A **14**, 3027–3039 (1966).
19. W. R. Dolbier, Jr. and W. F. Beach, "Parylene-AF4: a polymer with exceptional dielectric and thermal properties," J. Fluorine Chem. **122**, 97–104 (2003).
20. G. Duplâtre, M. F. Ferreira Marques, and M. da Graça Miguel, "Size of sodium dodecyl sulfate micelles in aqueous solutions as studied by positron annihilation lifetime spectroscopy," J. Phys. Chem. **100**, 16608–16612 (1996).
21. Curtis Write Surface Technologies, "Parylene coating services," 2010, http://www.paryleneinc.com/faq.php.
22. F. Mugele and J.-C. Baret, "Electrowetting: from basics to applications," J. Phys. **17**, R705–R774 (2005).
23. J. T. Gopinath, V. M. Bright, C. C. Cogswell, R. D. Niederriter, A. Watson, R. Zahreddine, and R. H. Cormack, "Simulation of electrowetting lens and prism arrays for wavefront compensation," Appl. Opt. **51**, 6618–6623 (2012).
24. S. Chevalliot, S. Kuiper, and J. Heikenfeld, "Experimental validation of the invariance of electrowetting contact angle saturation," J. Adhes. Sci. Technol. **26**, 1909–1930 (2011).
25. F. Krogmann, W. Mönch, and H. Zappe, "Electrowetting for tunable microoptics," J. Microelectromech. Syst. **17**, 1501–1512 (2008).
26. S. Diaham, M. Bechara, and M.-L. Locatelli, "Dielectric strength of Parylene HT," J. Appl. Phys. **115**, 054102 (2014).
27. P. Liebetraut, S. Petsch, J. Liebeskind, and H. Zappe, "Elastomeric lenses with tunable astigmatism," Light **2**, e98 (2013).
28. B. Berge, J. Broutin, H. Gaton, G. Malet, E. Simon, and F. Thieblemont, "Liquid lens based electrowetting: actual developments on larger aperture and multiple electrodes design for image stabilization or beam steering," Proc. SPIE **8616**, 861612 (2013).
29. V. N. Mahajan, "Zernike circle polynomials and optical aberrations of systems with circular pupils," Appl. Opt. **33**, 8121–8124 (1994).